An IGBT Turn-ON Concept Offering Low Losses Under Motor Drive *dv/dt* Constraints Based on Diode Current Adaption

Erik Velander, *Student Member, IEEE*, Lennart (Zdansky) Kruse, Thomas (Lundström) Wiik, Anders Wiberg, Juan Colmenares, *Student Member, IEEE*, and Hans-Peter Nee, *Senior Member, IEEE*

***Abstract*—In this paper, a new low-loss turn-ON concept for the silicon insulated-gate bipolar transistor (Si-IGBT) in combination with silicon p-i-n diode is presented. The concept is tailored for two-level motor converters in the 100 kW to 1 MW range under the constraint that the output voltages slopes are limited in order to protect the motor windings. Moreover, analyses of the IGBT turn-ON and diode reverse recovery voltage slopes are presented concluding that the diode reverse recovery is the worst case. The concept includes a low-cost measurement of the free-wheeling diode current and temperature by the gate driver without necessity of acquiring this information from the converter control board. By using this concept, the output *dv/dt* at the diode turn-OFF can be kept approximately constant regardless of the commutated current and junction temperature. Hence, the switching losses could be decreased for the currents and temperatures where the voltage slopes are lower when using a conventional gate driver optimized for the worst case. Moreover, results are shown for one such power semiconductor, showing a total switching loss reduction of up to 28% in comparison with a gate driver without current and temperature measurement. Finally, this concept is particularly suitable for high power semiconductor modules in half-bridge configuration which are recently proposed by several suppliers.**

***Index Terms*—AC motor drives, insulated gate bipolar transistors, power semiconductor devices.**

I. Introduction

CONSIDERING a two-level voltage source converters (VSCs) for motor drives in the 100 kW to 1 MW range, the silicon insulated-gate bipolar transistor (Si-IGBT) in combination with a silicon p-i-n diode is the current state-of-the art as power devices. In order to obtain high converter efficiency, enabling high converter power density and low junction temperatures, the switching losses must be kept low by fast switching of the IGBT, resulting in high current and voltage slopes. Reduced junction temperature is beneficial for converter life time [1]–[5], especially for applications with a varying load cycles, e.g., wind power, electrical hybrid vehicles, and train traction motor converters. The low switching losses can alternatively be utilized by using a higher switching frequency, resulting in reduction of the harmonic losses in the motor, which in turn increases the efficiency of the motor [6].

However, fast switching also results in high output voltage slopes (dv/dt) which potentially could result in significant voltage amplifications at the motor terminals as well as overvoltage of the first coil winding turns resulting in partial discharge and shorter life time of the motor [7]–[13].

This issue is especially pronounced in trains, where the traction converter is placed where space is available, e.g., on the roof, while the traction motors by necessity are placed in the bogies underneath the train. This arrangement concept could result in long feeding cables between the converter and the motor which potentially increases problems with voltage amplification [14], [15]. Moreover, high dv/dt is also a factor that can cause electromagnetic interference (EMI) in the gate-driver (GD) [16] and in the rest of the drive system [17]–[19]. The relationships between EMI levels and switching speeds are extensively described in [20].

One way to address the dv/dt issue is to include a filter at the inverter output or on the motor terminals as presented in [14] and [21]–[27]. However, these concepts require additional high voltage components which are costly, require space, add system losses, and are often very difficult to diagnose on-line in case of a failure. Consequently, a solution without a filter would be desired.

Moreover, the level of the output dv/dt is linked to commutated voltage and current as well as the junction temperature of the power device for the operating point. When using a conventional GD (CGD) [28] Si-IGBTs and p-i-n diodes often exhibit the highest dv/dt at very low current and temperature [29], [30], while they are most often used at moderate and high temperature and varying values of the current. If the CGD is adjusted to fulfill the required acceptable dv/dt constraint for the IGBT turn-ON/diode turn-OFF operation point with the highest dv/dt, i.e., at very low load current, higher currents will inevitably exhibit lower dv/dt. As a consequence, the switching losses at these higher currents will be unnecessarily high using the CGD and as a result, the total dissipation in the IGBT will be higher than necessary.

Manuscript received December 12, 2016; revised February 17, 2017; accepted March 20, 2017. Date of publication March 28, 2017; date of current version November 2, 2017. Recommended for publication by Associate Editor Luca Dalessandro. *(Corresponding author: Erik Velander.)*

E. Velander, L. (Zdansky) Kruse, T. (Lundström) Wiik, and A. Wiberg are with Bombardier Transportation, Västerås 72371, Sweden (e-mail: erik.velander@rail.bombardier.com; lennart.kruse@rail.bombardier.com; thomas.wiik@rail.bombardier.com; anders.wiberg@rail.bombardier.com).

J. Colmenares and H.-P. Nee are with the KTH Royal Institute of Technology, Stockholm 114 28, Sweden (e-mail: juanco@kth.se; hansi@kth.se).

Color versions of one or more of the figures in this paper are available online at http://ieeexplore.ieee.org.

Digital Object Identifier 10.1109/TPEL.2017.2688474

See http://www.ieee.org/publications_standards/publications/rights/index.html for more information.

In order to address this issue many different active gate drives have been proposed in order to actively adjust the current and voltage slopes of the IGBT. They can be divided into four different groups: open-loop concepts using different gate resistors, as proposed in [31]–[34]; gate currents, studied in [35]–[45]; gate voltages, presented in [46] and [47]; and finally closed-loop control principles, which are evaluated in [48]–[53].

However, the dv/dt constraints for a multiphase motor apply to the phase to phase voltage at the motor terminals. As a consequence, the terminals are exposed either to the voltage change across the diode (dv_{AC}/dt) or the IGBT (dv_{CE}/dt). Assuming that phases are commutated one at a time, there are two different kinds of transitions: IGBT turn-OFF, resulting in diode turn-ON, and IGBT turn-ON, resulting in diode reverse recovery (i.e., diode turn-OFF). For each of these kinds, the semiconductor part having the worst dv/dt will be limiting the maximum allowable switching speed.

For IGBT turn-OFF, the major part of the voltage transient, the rise of the collector-emitter voltage (v_{CE}) up to the dc-link level, takes place before the commutation of the current to the diode. Hence, there is no change to the dc-link current during the voltage rise and hence no induced voltage across the dc-link stray inductance. As a consequence, the transition rate in absolute terms of the diode turn-ON dv_{AC}/dt is equal to the one of the IGBT dv_{CE}/dt during this period. Hence, it can be concluded that a GD designed to fulfill the dv/dt constraint for the IGBT turn-OFF dv_{CE}/dt is sufficient to limit the motor terminal dv/dt also with respect to diode turn-ON.

However, for IGBT turn-ON, the diode voltage rise takes place during the reverse recovery current which depends on the operating point. As this current is changing during diode voltage rise, a voltage drop is induced in the dc-link stray inductance. As a result, dv_{AC}/dt is different from dv_{CE}/dt. Therefore, in a motor drive converter, both dv_{AC}/dt and dv_{CE}/dt must be considered when turning ON the IGBT. dv_{AC}/dt tends to be higher than dv_{CE}/dt, especially at low currents [54] and low temperatures [55]. This will be further described in Section II. A potential simple solution to this problem would be to add an RC-snubber across the diode in order to reduce the diode dv/dt without significantly affecting the semiconductor device switching losses [56]. However, significant additional losses are introduced in the snubber. Other drawbacks arise from the increased number of components in form of these resistors and capacitors: increased parts and assembly cost, increased space and decreased reliability.

When implementing a closed loop GD to control the diode reverse recovery dv_{AC}/dt the problem arises that the voltage across the diode is not at the same potential as the GD. In order solve this, the voltage information needs to be transferred between the GDs in real time. To accomplish this, a not easily realized communication link would be required, which would add cost and complexity and needs to be avoided. An alternative method to this demanding concept is an open loop control of the IGBT turn-ON process adapted to the commutated current and power switch temperature. These are quasi-constant parameters that may be measured and transmitted to the IGBT GD with a much lower bandwidth. One proposed way to implement this concept is to transmit the measured phase current level from the converter control board (CCB) to the GD and adapt the turn-ON control accordingly [57]. This proposal requires a separate input on the GD. For low-power low voltage VSCs with the drive units implemented on the same printed circuit board as the CCB, this can easily be realized by an additional short signal-path for each GD to serve this function. However, for high power applications, especially with high pollution degree requirements in traction and heavy equipment, the CCB is normally not placed nearby the GDs. As a result, this concept would require an additional signaling link, e.g., an optical link which adds cost, complexity, and production time.

Therefore, in this paper, a new IGBT turn-ON concept is proposed for high power ($\geq$100 kW) applications with an active current source GD with adaption to the diode freewheeling current by using a new simple diode current measuring concept. Contrary to what is presented in [57], this new measurement concept is built into the GD making it independent of current information from the CCB. Moreover, the new concept is particularly suitable for high-power semiconductor modules in half-bridge configuration, such as recently proposed by several suppliers [58]–[60]. This will be further described in Section III.

By using this concept, dv/dt for both the IGBT and the diode are kept below the maximum allowable value for all operating points without having unnecessarily low dv/dt and, consequently, high switching losses for most operating points. Moreover, this concept is tailored for a half-bridge gate drive unit (GDU), which is beneficial for the new half-bridge housing, and does not need any additional hardware interface to the CCB.

The relationship between the IGBT dv/dt and the diode dv/dt is analyzed in Section II, an overview of the concept is shown in Section III including the turn-ON execution scheme and the proposed diode current measurement circuit. Furthermore, the measurement results are shown in Section IV. Finally, a discussion is presented in Section V and Section VI concludes this paper.

II. Analysis of the Relationship Between IGBT and Diode dv/dt

This section describes the difference between dv/dt across the IGBT during turn-on and the dv/dt across the diode during its reverse recovery, which from experience is known to be higher.

In Fig. 1, an example of a diode turn-OFF is shown with an inductive load and the diode connected to the negative terminal of the dc-link. The upper diode and the lower IGBT are omitted as they are not influencing the turn-ON of the upper IGBT in case that the load current is going out of the phase. Moreover, L_σ is the dc-link stray inductance, C_{RES} is the IGBT reverse transfer capacitance, C_{GE} is the IGBT gate-emitter capacitance, i_G is the gate current, v_{AC} is the diode voltage, and v_{CE} is the collector–emitter voltage of the IGBT.

The dc-link voltage V_{DC} and the load current I_L are assumed to be constant during the commutation process as the load is highly inductive. Therefore, two conclusions can be drawn. First, the load voltage is in this case assumed to be approxi-

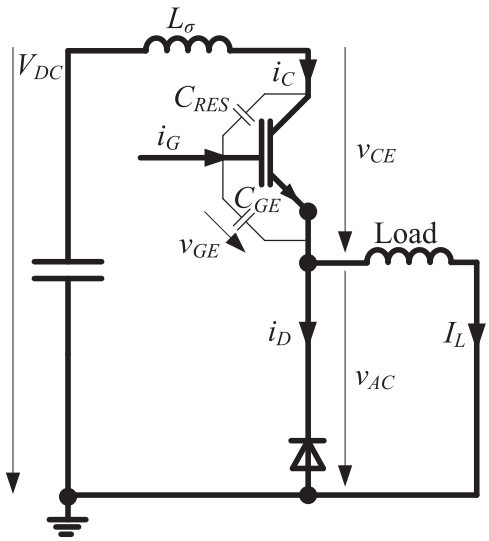

Fig. 1. Illustration of two-level phase leg with a p-i-n diode and a silicon IGBT with dc-link stray inductance.

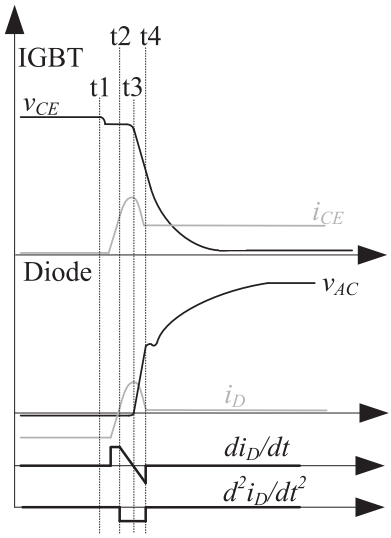

Fig. 2. Illustration of voltages and currents across the IGBT and the diode during diode turn-OFF.

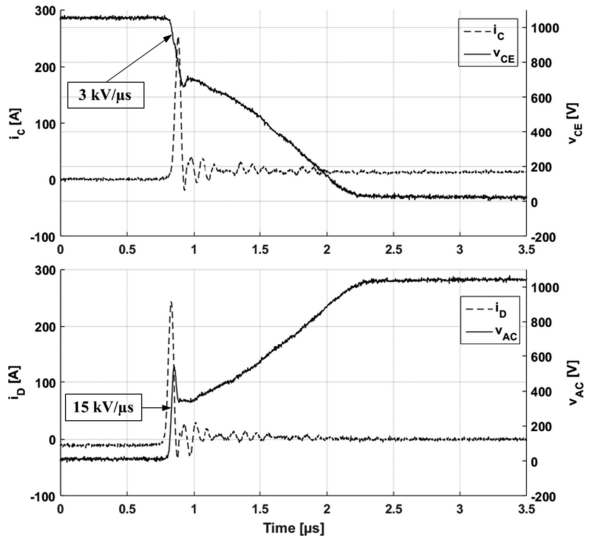

Fig. 3. Measured IGBT turn-ON and diode turn-OFF at 10 A and 1050 V in order to illustrate di_C/dt, $dv_{\rm CE}/dt$, di_D/dt, and $dv_{\rm AC}/dt$.

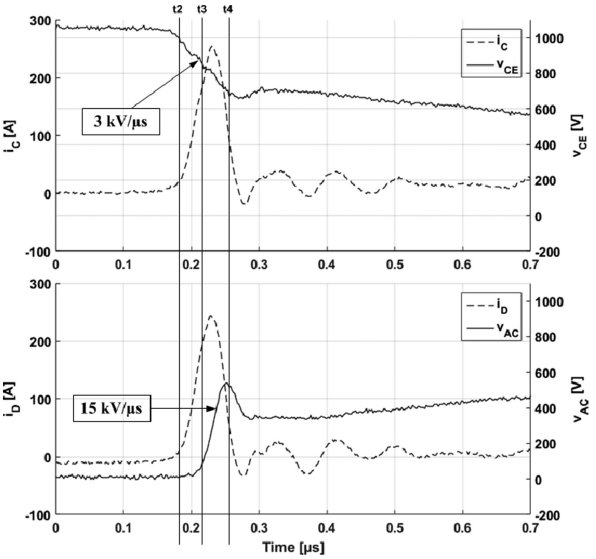

Fig. 4. Same measurement as Fig. 3 in order to illustrate di_C/dt, $dv_{\rm CE}/dt$, di_D/dt, and $dv_{\rm AC}/dt$, but with focus on the diode reverse recovery with marked time events from Fig. 3.

mately equal to diode voltage as shown in Fig. 1 as most of the contribution to L_σ is caused by the capacitor and the busbar. As a second conclusion, di_D/dt can be concluded to be equal to di_C/dt.

Moreover, the voltages shown in Fig. 1 can be expressed as

$$V_{\rm DC} = L_\sigma \frac{di_D}{dt} + v_{\rm CE} + v_{\rm AC}. \tag{1}$$

As a result, the voltage slopes can be expressed as

$$\frac{dv_{\rm AC}}{dt} = -L_\sigma \frac{d^2 i_D}{dt^2} - \frac{dv_{\rm CE}}{dt}. \tag{2}$$

As seen in (2), $dv_{\rm AC}/dt$ is different from $dv_{\rm CE}/dt$ while the reverse recovery process is active and the diode current is changing. In Fig. 2 the IGBT turn-ON and diode turn-OFF voltages and currents are illustrated for a typical IGBT and diode combination. As the voltage across the diode starts to increase close to the peak of the reverse recovery current (t3 in Fig. 2), the second derivate $d^2 i_D/dt^2$ determines $dv_{\rm AC}/dt$ from $dv_{\rm CE}/dt$ according to (2). Since both $d^2 i_D/dt^2$ and $dv_{\rm CE}/dt$ are negative in the time interval t3 to t4, $dv_{\rm AC}/dt$ must have higher amplitude than $dv_{\rm CE}/dt$ according to (2).

In Figs. 3 and 4, measured waveforms are shown for $dv_{\rm CE}/dt$ and $dv_{\rm AC}/dt$, respectively, using the same semiconductor and GD type. As seen clearly, $dv_{\rm AC}/dt$ is significantly higher, about 15 kV/μs, than $dv_{\rm CE}/dt$ which is about 3 kV/μs as long as the reverse recovery process is active. In Fig. 4, the time marks from Fig. 2 are inserted in order to illustrate the different process steps in time.

Thus, $dv_{\rm AC}/dt$ is found to be higher than $dv_{\rm CE}/dt$ during the reverse recovery.

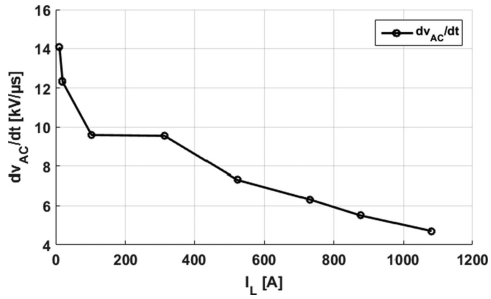

Fig. 5. Diode $dv_{\rm AC}/dt$ during the reverse recovery process as a function of I_L for commutating to an IGBT using a constant I_G for the same dc-link voltage, I_G, and junction temperature.

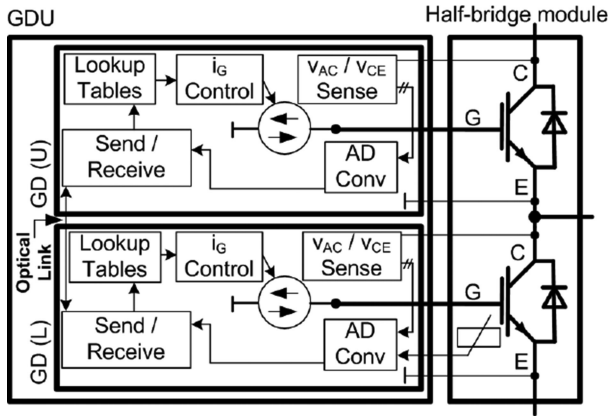

Fig. 6. Proposed GDU concept with a half-bridge module configuration with a GD controlling each IGBT.

However, by controlling the IGBT gate, $di_{\rm CE}/dt$ and $dv_{\rm CE}/dt$ can be controlled [61]. By using a constant I_G, $dv_{\rm CE}/dt$ can be controlled independently of I_L [40].

Moreover, $dv_{\rm AC}/dt$ is dependent on $dv_{\rm CE}/dt$ as described (2), but also on d^2i_D/dt^2. The shape of i_D is a result of the diode design, di_D/dt, and the magnitude of I_L [62]. Therefore, even if $dv_{\rm CE}/dt$ is independent of I_L, $dv_{\rm AC}/dt$ during the reverse recovery is dependent on I_L. The reason is that the initially stored charge in the diode is dependent on I_L. Therefore, at low values of I_L, $dv_{\rm AC}/dt$ is higher than at high values of I_L [29]. This is illustrated in Fig. 5 where $dv_{\rm AC}/dt$ during the reverse recovery is shown as a function of I_L. During these measurements, a time-constant I_G with the same value is used for all measured points. As seen, for low currents, $dv_{\rm AC}/dt$ is more than 10 kV/μs while the values for higher currents are below 5 kV/μs, which is expected from the conclusions drawn in [29] and [30].

Moreover, as the current output of the VSC is sinusoidal, the GD must be adjusted to fulfill dv/dt constraint for the smallest current, resulting in unnecessarily high losses at high currents where dv/dt is significantly lower.

Therefore, a new concept with the i_G execution scheme adapted to I_L is presented in the next section.

III. Description of the Loss Effective Diode-Current-Dependent IGBT Turn-ON (LED-IT) Concept

On the top of the new high-power semiconductor modules in half-bridge configuration, between the dc and the phase connections, there are dedicated spaces for mounting the GDU. As a consequence, it is particularly attractive to design half-bridge GDUs divided into two GDs, one for the upper IGBT position and one for the lower.

An overview of the loss effective diode-current-dependent IGBT turn-ON (LED-IT) concept, incorporated in such GDU, is shown in Fig. 6. Moreover, one field programmable gate array (FPGA) with a read-only memory serves as a controller on each GD. The GD attached to the lower IGBT measures the temperature using the built-in temperature sensor and both GDs measure the diode forward voltage drop. This voltage drop serves as a measure of I_L which is more described in Section III-B.

The new half-bridge module configuration makes the physical distance between GDs short. As a consequence, a short communication link between the lower and upper position GDs can replace a separate optical fiber link from the CCB to the upper GD. The number of optical fibers interfacing with the CCB could then be reduced by half. This saves manufacturing time and component costs. In addition, as this link is available, it can also be used for additional data. In the proposed LED-IT concept, this is utilized for transferring the temperature and forward voltage drop data between the two GDs. As a result, there is no extra physical communication line needed for the LED-IT concept.

When using this concept, the look-up tables for each particular application (IGBT and diode types, commutation inductance, voltage, current and temperature ranges, and the allowable dv/dt) must be established by series of measurements of dv/dt and the sampled input diode forward voltage drop. These series must cover all temperatures, currents, and dc-link voltage levels. By doing so, a set of gate drive parameters can be found that optimizes the switching losses under the dv/dt constraint. The optimized parameters are subsequently stored in the look-up table of the control FPGA under the sampled input parameter values. As a result, the gate current can be adjusted so that the required dv/dt level at the diode is not exceeded for any commutated current.

Moreover, the IGBT turn-on scheme, using the current sources, and the measurement circuit for $v_{\rm AC}$ are explained in Sections III-A and III-B.

A. IGBT Turn-ON Scheme for the LED-IT Concept

The proposed turn-ON scheme, as shown in Fig. 7, uses intervals each with constant gate current as also proposed in the literature [38], [45]. The levels are predefined and adjusted for the semiconductor type for which the concept is used with.

During the first interval, 1, a reasonably high precharge current is used in order to raise $v_{\rm GE}$ from –15 V to approximately 0 V in order to reduce the total turn-ON delay. The level and time duration in this interval are precalibrated with fixed values

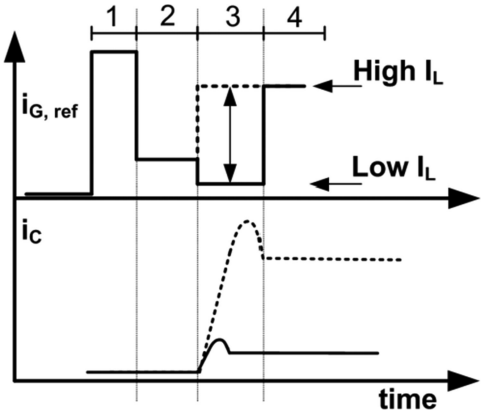

Fig. 7. LED-IT turn-ON scheme.

for each IGBT type. During interval 2, i_G is adjusted to a lower value until a measurable value of di_C/dt is detected by sensing voltage drop between the emitter main and kelvin terminals. The level of i_G in this interval must be high enough to avoid a long delay, but low enough to be able to change the level quickly to the lower value which is precalibrated for a low value of I_L. The voltage drop between the emitter main and kelvin terminals can easily be measured by the GD as proposed in [33] and [53]. For interval 3, i_G is selected from a table, stored in read-only-memory on the GD. When selecting the value from the table, the received forward diode voltage from the complementary switch is used. This voltage is an estimate of I_L and has been measured by the complementary switch and transferred by the optical link, shown in Fig. 6, prior to the turn-ON process. The table itself is programmed into the read-only-memory. The value of i_G which is looked-up from the measured diode forward voltage has been precalibrated to give the optimal $dv_{\rm AC}/dt$ over the diode at this I_L for the worst case temperature and dc-link voltage. The duration of this interval is also precalibrated long enough to last during the i_C rise and the reverse recovery for this particular power device. In the subsequent interval 4, i_G has a higher, fixed value in order to keep the IGBT turn-ON loss low by charging the Miller capacitance at a higher rate. During this time interval, $dv_{\rm CE}/dt$ is the same as $dv_{\rm AC}/dt$ and there is therefore no need to adapt i_G with respect to I_L any more. As the last step, a MOSFET stage and a resistor are activated to hold the gate at $+15$ V.

By using this concept, $dv_{\rm AC}/dt$ can be controlled to a constant value, independent of I_L. As a result, the losses can be kept low at high currents and $dv_{\rm AC}/dt$ can be kept at acceptable levels at low currents.

For low temperatures, which pertain to the warm-up period of the converter, a fixed, low value of i_G is used in interval 3, adjusted to fulfill the $dv_{\rm AC}/dt$ requirement for low values of I_L. This means that $dv_{\rm AC}/dt$ is lower for high values of I_L as illustrated in Fig. 5. The benefit of doing so is that the p-i-n diode voltage variations with temperature is less significant to the concept as the measurement setup is only used for warm temperatures. The temperature threshold can be adjusted by a parameter in the memory.

B. Freewheeling Diode Forward Voltage Measurement on the GD

In order to adapt i_G with respect to I_L during the IGBT turn-ON, a cost-effective current measurement concept is proposed. Before the turn-ON, during the freewheeling interval, I_L causes a forward voltage drop on the complementary diode. This voltage drop can be measured by the GD.

The diode voltage drop during the freewheeling interval is a result of the diode junction built-in potential of approximately 0.8 V and a resistive part of approximately 1–1.5 V, which corresponds mainly to the voltage drop across the drift region. The built-in potential is dependent on temperature, but not dependent on I_L. As the concept is used within a limited temperature range, the contribution of this part can be removed using a GD temperature-dependent offset in the look-up table for the built-in potential. On the other hand, the resistive part is current and temperature dependent and could be utilized for current estimation in this limited temperature range. Moreover, there is an inductive part caused by the module parasitic inductance L_D. This inductive voltage contribution can be calculated as

$$v_{D,\rm ind} = L_D \frac{di_L}{dt} \tag{3}$$

where di_L/dt is the current change rate of the freewheeling traction motor phase current. di_L/dt is the highest when the full dc-link voltage U_W is applied across the machine inductance. An example is during traction when the speed of the motor is the highest or in braking at low speed. During those cases, the induced voltage across the diode can be calculated using the phase load inductance L_W as

$$\frac{di_D}{dt} = \frac{U_W}{L_W}. \tag{4}$$

Reasonable values for U_W and L_W are 1 kV and 1 mH, respectively, resulting in a change rate of 1 A/μs using (4). As a result, the maximum diode inductive voltage can be concluded to be 5 mV using (3) if L_D is 5 nH. This inductive voltage drop can be considered to be negligible since it constitutes less than 1% of current-dependent diode forward voltage drop (1–1.5 V). The inductive voltage drop is, therefore, omitted from this study as it focuses on the new high power half-bridge housing with auxiliary terminal connectors. As those connectors are used, the stray inductance voltage drop in the bond-wires connecting the main terminals and dies together does not contribute to the measured voltage. For other applications, e.g., an industrial motor drive with MOSFETs using the TO-247 package where the sense terminals are not available, the inductive voltage drop might be of greater significance.

An overview of the measurement circuit in the GD is shown in Fig. 8. The diode voltage measurement circuit consists of a current source, a resistor, and a chain of diodes in order to measure the diode forward voltage using the auxiliary terminals. This concept is well known to be used also for short-circuit detection for various devices [63]. In order to avoid inductive feedback to the gate control, the GD is connected to the collector and emitter "sense" terminals, which have connections very close to the semiconductor chips.

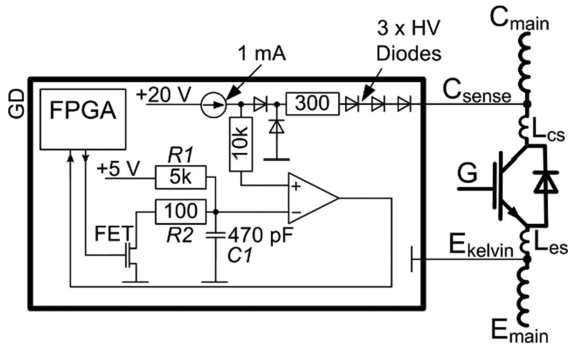

Fig. 8. Simplified overview of GD with the proposed forward voltage drop measurement circuit.

For analog-to-digital conversation (ADC) of the measured forward voltage drop, a new cost-effective implementation is proposed. This concept uses a fast comparator, a simple small signal MOSFET, the resistors $R1$, $R2$, and the capacitor $C1$ to build up a charging circuit used to convert the analog forward voltage to a digital value as shown in Fig. 8. For each measured sample, $C1$ is charged through $R1$. When the voltage of $C1$ exceeds the voltage from the diode voltage measurement circuit, the comparator changes its output. The time duration from start of charging $C1$ to the change of the comparator output is then recorded. This time duration is used a measure of the diode voltage drop as a digital value. The accuracy of this measurement is approximately 2%. Before the next sample, the FET and $R2$ are used in order to discharge $C1$. The maximum ADC sampling frequency f_s can be calculated from the rise time t_r of the charging circuit and the discharge time t_d as

$$t_r = 2.2 \cdot R1 \cdot C1, \tag{5}$$

$$t_d = 2.2 \cdot R2 \cdot C1, \tag{6}$$

$$T_s = \frac{1}{f_s} = t_r + t_d. \tag{7}$$

The $R1$, $R2$, and $C1$ values proposed are 5 kΩ, 100 Ω, and 470 pF, respectively, resulting in a minimum sampling time of 5.3 μs. For Si p-i-n diodes, the conductivity modulation requires the minimum ON-time to be at least in the order of 10 μs, otherwise the reverse recovery is also strongly dependent on the ON time [64]. However, by using the proposed values, at least one sample is received for each freewheeling time period.

By using this charging circuit, the necessity of a cost-driving analog-to-digital converter and a potentially needed signal operation amplifier could be avoided. Moreover, the often used short-circuit protection strategy by measuring the IGBT saturation voltage can share the same circuitry and components. For short-circuit detection, a single comparator port could be used instead of the charging circuit as an input to the FPGA in order to compare the measured IGBT saturation voltage with a reference level [65].

Moreover, the diode chain voltage drop is temperature dependent, a temperature difference in the diode chain of 10 K corresponds to a measurement error of approximately 75 mV in the p-i-n power diode voltage measurement and 100 A in the freewheeling current. Therefore, in order to avoid a significant influence of diode chain temperature, the temperature of the GD can be measured and used for compensation in the look-up table. An alternative solution can be to include a compensating similar diode chain in the reference voltage network of the v_F measurement.

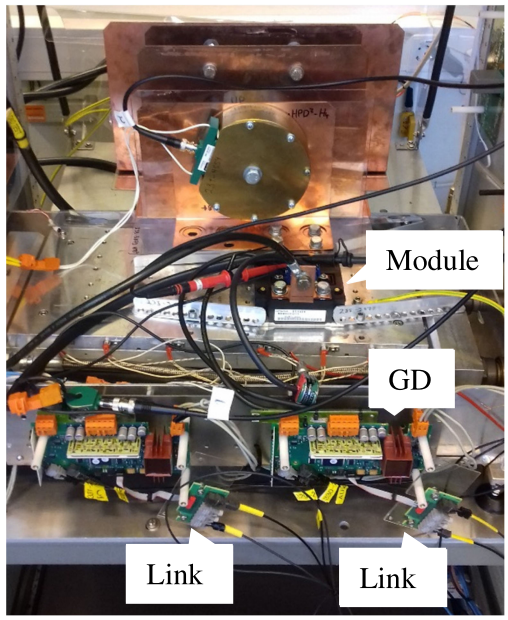

Fig. 9. Photo of the experimental setup.

IV. Experimental Results

Two GDs were prototyped with the proposed analog-to-digital measurement circuit, one for each IGBT in the half-bridge phase leg. In addition, the intercommunication between the GDs was realized by one optical link in each direction using a universal asynchronous protocol in order to transmit the measured v_{AC}.

The IGBT module used for the evaluation is Hitachi MBM900FS17F [66] and is rated 900 A and 1700 V.

For all measurements, a standard double-pulse test setup was used. The total dc-link inductance L_σ was found to be 30 nH including the half-bridge module, as well as the holder for the Pearson 4997 current measurement probe and the capacitors. For the i_G measurement, a Pearson 2878 was used. Moreover, air inductors served as loads and the module baseplate were heated by a heating element and connected to a thermocouple for the temperature recording. Passive voltage probes with a bandwidth of 200 MHz were used for the v_{CE}, v_{AC}, and v_{GE} measurements. In all tests, the lower position was measured. In Fig. 9, the experimental setup is shown. In the photo, the optical components used in order to verify the function of the communication link between the upper and lower GDs are clearly indicated with "link."

Moreover, as concluded in the previous section, the LED-IT concept allows dv_{AC}/dt to be adjusted by firmware to meet the actual requirement for a certain application. However, for these

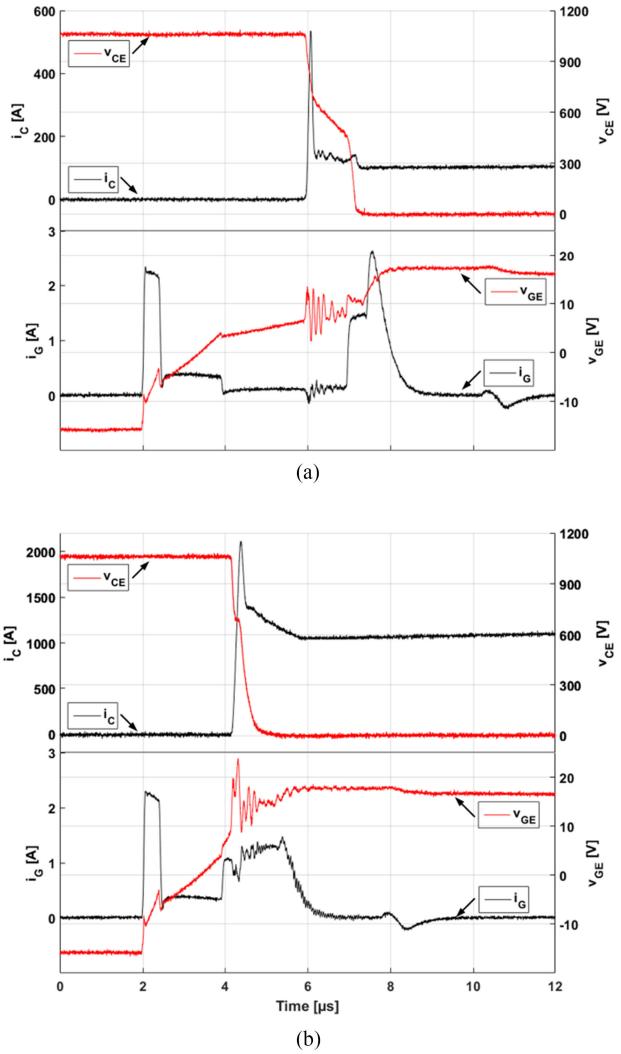

Fig. 10. Waveforms of the IGBT using LED-IT concept at 1050 V and 100 A (a) and 1100 A (b) using the same time axis.

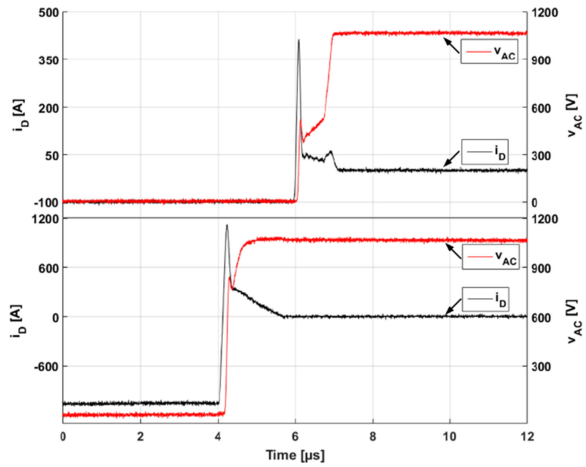

Fig. 11. Waveforms of the p-i-n diode using the LED-IT concept at 1050 V and 100 A (upper graph) and 1100 A (lower graph) using the same time axis.

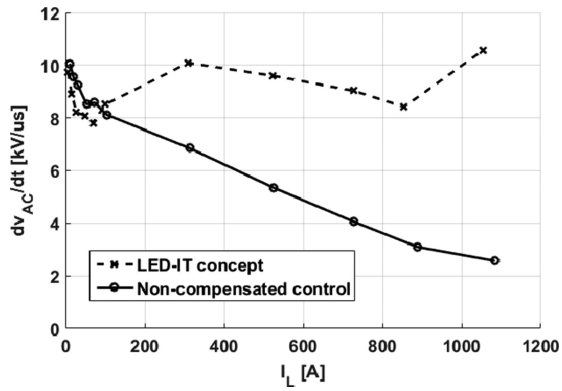

Fig. 12. Comparison of the diode turn-OFF dv_{AC}/dt between the LED-IT concept and non-compensated control at 60 °C and 1050 V.

measurements, a value of 10 kV/μs was used in order to verify the function and the performance of the concept.

Measurements with the LED-IT concept are shown in the next section. As a reference, a control method using a fixed i_G value during interval 3 in Fig. 7 is used, hereafter called noncompensated control.

In order to verify the LED-IT scheme, recorded waveforms are shown for 100 A in Fig. 10(a) and 1100 A in Fig. 10(b). As seen in the figures, i_G is similar in (a) and (b) before i_C starts to rise which corresponds to intervals 1 and 2 in Fig. 7. Later on, at 4 μs, i_G is adjusted with respect to the current which is measured and transferred from the upper GD by the optical link. As seen in the graphs, i_G is approximately 100 mA at this point for the 100 A case (a) and approximately 1 A for the 1100 A case (b). The currents in intervals 2 and 3, see Fig. 7, are precalibrated to be equal for the 100 A case for this particular power device. The time duration of interval 4 is fixed to cover the current rise and reverse recovery for all operation points as stated in Section III. As a result, for low I_L, dv_{CE}/dt is unnecessarily low after the reverse recovery of the diode as seen in Fig. 10. However, these extra losses due to this limitation at low I_L constitute only a fraction of the total losses when using the converter for all currents as can be seen in Fig. 13.

Moreover, the corresponding graphs for the p-i-n diode are shown in Fig. 11 using the same setup as in Fig. 10.

A. Comparison of dv/dt of the Noncompensated Control and LED-IT

In Fig. 12, the worst case recorded dv_{AC}/dt is shown as a function of commutated current using the same setup. The worst case was found to be at the lowest junction temperature and highest dc-link voltage, 60 °C and 1050 V, respectively. For higher temperatures, up to 125 °C and lower dc-link voltages, down to 750 V, dv_{AC}/dt was found to be slightly lower using the same concept, settings, and component. As seen in the figure, the highest values are occurring at low commutated current using the noncompensated control. However, at higher currents, dv_{AC}/dt values are significantly lower, about 2.5 kV/ μs at 1100 A. This leads to unnecessarily high switching losses for the IGBT at this operating point. On the other hand, when the LED-IT concept is used, dv_{AC}/dt can be adjusted with respect to the current,

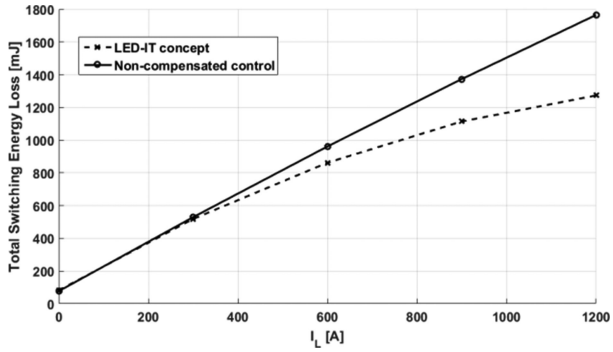

Fig. 13. Comparison of the total switching loss between the LED-IT concept and the noncompensated at 125 °C and 1050 V.

resulting in almost constant $dv_{\rm AC}/dt$ and reduced switching losses.

B. Comparison of the Switching Losses of the Noncompensated Control and LED-IT

In this section, the switching loss performances are compared using the LED-IT concept as well as the noncompensated control. In order to present an input for converter performance evaluation, the total switching losses are compared (IGBT turn-OFF, IGBT turn-ON, and the diode reverse recovery).

The IGBT losses have been calculated using the well-known power loss integral for the IGBT

$$E_{\rm ON,OFF} = \int_0^{t_W} v_{\rm CE} \cdot i_C dt \tag{8}$$

where t_W is the entire time duration of the switching event and $v_{\rm CE}$ and i_C are the measured voltage and currents with the steady-state offsets subtracted. For the diode reverse recovery losses, the corresponding equation is

$$E_{\rm REC} = \int_0^{t_W} v_{\rm AC} \cdot i_D dt. \tag{9}$$

For the IGBT turn-OFF loss measurement, the current source based control was used using the same hardware as for the IGBT turn-ON evaluation. However, the switching behavior and the losses using this method at IGBT turn-OFF were found to be the same as by using the CGD with the datasheet RG-value.

The total switching losses are similar for the lower current range for the noncompensated GD and the LED-IT concept as shown in Fig. 13. For these measurements, the losses were recorded at a temperature of 125 °C. At this temperature, the switching losses are higher than at 60 °C for which $dv_{\rm AC}/dt$ were recorded and presented in Fig. 12. However, the same setup was used during both measurements.

In Table I, the resulting loss reduction using the proposed control is presented. As seen, the benefit, in terms of switching loss reduction, of the LED-IT concept is higher for higher currents than for lower currents. As a result, the LED-IT concept is more beneficial when the converter is heavily loaded.

TABLE I
LOSS IMPROVEMENT OF LED-IT CONCEPT AT 1050 V FOR MAX 10 kV/μs

	600 A	900 A	1200 A
Improvement of total switching loss $E_{\rm on} + E_{\rm off} + E_{\rm rr}$	10%	19%	28%

V. DISCUSSION

In this paper, a new programmable logic-based universal GD hardware concept for measuring the diode freewheeling current and adapting the IGBT turn-ON for optimization of switching losses under an application imposed dv/dt constraint is presented. For motor drive applications, e.g., railway traction, dv/dt for the diode turn-OFF is a limiting design parameter in order to avoid pre-aging due to partial discharge between the windings in the motor. As the p-i-n diode $dv_{\rm AC}/dt$ is lower for higher currents, where the IGBT switching losses are the highest, there is a motivation to adapt the IGBT turn-ON to the actual current such that the losses are not higher than necessary given a certain application diode $dv_{\rm AC}/dt$ requirement. By doing so, the losses could be reduced by up to 28%. Based on the results, the LED-IT concept could lead to a junction temperature reduction of approximately 3–5 °C when operating in a train. Moreover, based on this temperature reduction, an estimated improvement of 20% in power thermal load cycling life time can be expected. For 3.3 or 6.5 kV devices, which are also often used for traction converters, the benefit of using the proposed concept is potentially higher as the switching losses, for these voltage levels, constitute a greater part.

In principle, this concept could also be used for a multilevel converter. However, the higher number of switches and, thus, GDs per phase in those converters makes it difficult to realize the communication between each GD connected to a diode and all GDs for IGBTs to which the diode current may commutate. In some multilevel converters, e.g., the neutral-point clamped (NPC) converter, there are not even GDs associated with all diodes and consequently no low-cost measurement of the freewheeling diode current. As a result this concept is less attractive for multilevel converters.

Moreover, the LED-IT measurement circuit and the commutation protocol must be fast, in the order of microseconds as the shortest conduction time of the diode is of the order of 10 μs. This bandwidth requirement may result in increased fault-tolerance sensitivity resulting in lost samples. In such case, a default i_G value can be used for the next commutation. As a result, this commutation exhibits a slightly higher switching loss. However, the resulting increase of the total switching loss over time would be negligible.

VI. CONCLUSION

In this paper, results for a low loss IGBT turn-ON concept under motor drive dv/dt constraint based on a current source based GDU has been presented. It consists of two intercommunicating GDs, one for the upper and one for the lower IGBT. Moreover, the p-i-n diode freewheeling current is estimated by

measuring the ON-state voltage drop and the temperature of the power module on the GD. By doing so, the turn-ON can be adjusted with respect to the current and temperature. As a result, the phase output dv/dt can be limited at the worst points without having unnecessarily high losses during the entire load cycle.

A detailed description was also given how the phase output dv/dt is linked to the GD and the commutation circuit in motor-drive application. In this description, it was found that diode-OFF dv/dt is a more severe case regarding phase output dv/dt than the IGBT turn-ON case. Moreover, the IGBT turn-OFF control was found to be sufficient in order to limit also the diode turn-ON dv/dt.

Additionally, a new cost-effective forward voltage measurement circuit is proposed based on a standard short-circuit protection circuit. By using the proposed circuit, the measurement shows that this estimation can be performed and the IGBT turn-ON process could be adapted accordingly.

Finally, the results show that the diode dv/dt at the turn-OFF could be adapted to the diode current by measuring it with the GD. The resulting diode turn-OFF dv/dt is independent of the commutated current resulting in a total switching loss reduction up to 28% compared to a noncompensated GD configured for the worst case diode turn-OFF dv/dt.

REFERENCES

[1] H. Huang and P. A. Mawby, "A lifetime estimation technique for voltage source inverters," *IEEE Trans. Power Electron.*, vol. 28, no. 8, pp. 4113–4119, Aug. 2013.

[2] D. Astigarraga *et al.*, "Analysis of the results of accelerated aging tests in insulated gate bipolar transistors," *IEEE Trans. Power Electron.*, vol. 31, no. 11, pp. 7953–7962, Nov. 2016.

[3] K. B. Pedersen and K. Pedersen, "Dynamic modeling method of electro-thermo-mechanical degradation in IGBT modules," *IEEE Trans. Power Electron.*, vol. 31, no. 2, pp. 975–986, Feb. 2016.

[4] L. Gopi Reddy, L. Tolbert, and B. Ozpineci, "Power cycle testing of power switches: A literature survey," *IEEE Trans. Power Electron.*, vol. 30, no. 5, pp. 2465–2473, May 2015.

[5] K. Ma, M. Liserre, F. Blaabjerg, and T. Kerekes, "Thermal loading and lifetime estimation for power device considering mission profiles in wind power converter," *IEEE Trans. Power Electron.*, vol. 30, no. 2, pp. 590–602, Feb. 2015.

[6] L. Tong, G. Wu, F. W. W. Shu, and E. He, "Influence of the inverter characteristics on the harmonic losses in PWM fed traction motors," in *Proc. Int. Symp. Electr. Insul. Mater.*, Jun. 2005, pp. 1–22.

[7] E. Persson, "Transient effects in application of PWM inverters to induction motors," *IEEE Trans. Ind. Appl.*, vol. 28, no. 5, pp. 1095–1101, May 1992.

[8] J. C. Wheeler, "Effects of converter pulses on the electrical insulation in low and medium voltage motors," *IEEE Electr. Insul. Mag.*, vol. 21, no. 2, pp. 22–29, Apr. 2005.

[9] M. Melfi, A. J. Sung, S. Bell, and G. L. Skibinski, "Effect of surge voltage risetime on the insulation of low-voltage machines fed by PWM converters," *IEEE Trans. Ind. Appl.*, vol. 34, no. 4, pp. 766–775, Aug. 1998.

[10] G. Skibinski, J. Erdman, J. Pankau, and J. Campbell, "Assessing ac motor dielectric withstand capability to reflected voltage stress using corona testing," in *Proc. IEEE IAS Electr. Mach. Conf.*, vol. 1, 1996, pp. 694–702.

[11] M. J. Melfi, "Low-voltage PWM inverter-fed motor insulation issues," *IEEE Trans. Ind. Appl.*, vol. 42, no. 1, pp. 128–133, Jan. 2006.

[12] M. Kaufhold, H. Aninger, M. Berth, J. Speck, and M. Eberhardt, "Electrical stress and failure mechanism of the winding insulation in PWM-inverter-fed low-voltage induction motors," *IEEE Trans. Ind. Electron.*, vol. 47, no. 2, pp. 396–402, Apr. 2000.

[13] T. Humiston and P. Pillay, "Parameter measurements to study surge propagation in induction machines," *IEEE Trans. Ind. Appl.*, vol. 40, no. 5, pp. 1341–1348, Sep. 2004.

[14] K. K.-F. Yuen and H. S.-H. Chung, "A low-loss 'RL-plus-C' filter for overvoltage suppression in inverter-fed drive system with long motor cable," *IEEE Trans. Power Electron.*, vol. 30, no. 4, pp. 2167–2181, Apr. 2015.

[15] A. F. Moreira, T. A. Lipo, G. Venkataramanan, and S. Bernet, "High-frequency modeling for cable and induction motor overvoltage studies in long cable drives," *IEEE Trans. Ind. Appl.*, vol. 38, no. 5, pp. 1297–1306, Sep. 2002.

[16] V.-S. Nguyen, L. Kerachev, P. Lefranc, and J. C. Crebier, "Characterization and analysis of an innovative gate driver and power supplies architecture for HF power devices with high dv/dt," *IEEE Trans. Power Electron.*, vol. 32, no. 8, pp. 6079–6090, Aug. 2017.

[17] T. Rahimi, S. Y. Khangah, and B. Yousefi, "Reduction EMI due to di/dt and dv/dt dc and ac sides of BLDC motor drive," in *Proc. 2014 5th Power Electron., Drive Syst. Technol. Conf.*, 2014, pp. 428–433.

[18] N. Mousavi, T. Rahimi, and H. M. Kelk, "Reduction EMI of BLDC motor drive based on software analysis," *Adv. Mater. Sci. Eng.*, vol. 2016, pp. 1–9, 2016.

[19] H. Riazmontazer and S. K. Mazumder, "Optically switched-drive-based unified independent dv/dt and di/dt control for turn-off transition of power MOSFETs," *IEEE Trans. Power Electron.*, vol. 30, no. 4, pp. 2338–2349, Apr. 2015.

[20] N. Oswald, P. Anthony, N. McNeill, and B. H. Stark, "An experimental investigation of the tradeoff between switching losses and EMI generation with hard-switched all-Si, Si-SiC, and all-SiC device combinations," *IEEE Trans. Power Electron.*, vol. 29, no. 5, pp. 2393–2407, May 2014.

[21] R. Mini, S. R. Resna, and M. N. Dinesh, "LC clamp filter for voltage reflection due to long cable in induction motor drives," in *Proc. Int. Conf. Emerging Res. Areas: Magn., Mach. Drives*, 2014, pp. 1–6.

[22] Y. Jiang, X. Chen, and D. Xu, "Research on a novel inverter output passive filter for reducing dv/dt at motor terminals in a PWM drive system," in *Proc. 6th Int. Conf. Electr. Mach. Syst.*, 2003, pp. 436–439.

[23] K. K.-F. Yuen, H. S.-H. Chung, and V. S.-P. Cheung, "An active low-loss motor terminal filter for overvoltage suppression and common-mode current reduction," *IEEE Trans. Power Electron.*, vol. 27, no. 7, pp. 3158–3172, Jul. 2012.

[24] P. Mart-ro, W. Sae-Kok, and S. Khomfoi, "Analysis of dv/dt filter installation for PWM ac drive applications," in *Proc. 2011 IEEE 9th Int. Conf. Power Electron. Drive Syst.*, 2011, pp. 177–184.

[25] W. Wu, Y. Jiang, Y. Liu, M. Huang, Y. He, and S.-H. Chung, "A new passive filter design method for overvoltage suppression and bearing currents mitigation in a long cable based PWM," in *Proc. 2016 IEEE 8th Int. Power Electron. Motion Control Conf.*, 2016, pp. 3103–3110.

[26] Q. Chang, Q. Ge, and B. Zhang, "A novel filter design approach for mitigating motor terminal overvoltage in long cable PWM drives," in *Proc. 9th IEEE Conf. Ind. Electron. Appl.*, 2014, pp. 1798–1803.

[27] A. von Jouanne and P. N. Enjeti, "Design considerations for an inverter output filter to mitigate the effects of long motor leads in ASD applications," *IEEE Trans. Ind. Appl.*, vol. 33, no. 5, pp. 1138–1145, Oct. 1997.

[28] A. R. Hefner, "An investigation of the drive circuit requirements for the power insulated gate bipolar transistor (IGBT)," *IEEE Trans. Power Electron.*, vol. 6, no. 2, pp. 208–219, Apr. 1991.

[29] H. Feng, W. Yang, Y. Onozawa, T. Yoshimura, A. Tamenori, and J. K. O. Sin, "Transient turn-on characteristics of the Fin p-Body IGBT," *IEEE Trans. Electron Devices*, vol. 62, no. 8, pp. 2555–2561, Aug. 2015.

[30] M. Honsberg, T. Radke, K. Ishii, and J. Manotobu, "A 6-in-1 IGBT module performance evaluation platform determining the trade-off between dv/dt and turn-on loss of different IGBT / FwDi chip setups," in *Proc. 2011 14th Eur. Conf. Power Electron. Appl.*, 2011, pp. 1–7.

[31] C. Licitra, S. Musumeci, A. Raciti, A. U. Galluzzo, R. Letor, and M. Melito, "A new driving circuit for IGBT devices," *IEEE Trans. Power Electron.*, vol. 10, no. 3, pp. 373–378, May 1995.

[32] R. Hemmer, "Intelligent IGBT drivers with exceptional driving and protection features," in *Proc. 2009 13th Eur. Conf. Power Electron. Appl.*, 2009, pp. 1–4.

[33] Z. Wang, X. Shi, L. M. Tolbert, F. Wang, and B. J. Blalock, "A di/dt feedback-based active gate driver for smart switching and fast overcurrent protection of IGBT modules," *IEEE Trans. Power Electron.*, vol. 29, no. 7, pp. 3720–3732, Jul. 2014.

[34] S. Musumeci, A. Raciti, A. Testa, A. Galluzzo, and M. Melito, "Switching-behavior improvement of insulated gate-controlled devices," *IEEE Trans. Power Electron.*, vol. 12, no. 4, pp. 645–653, Jul. 1997.

[35] V. John, B.-S. Suh, and T. A. Lipo, "High-performance active gate drive for high-power IGBT's," *IEEE Trans. Ind. Appl.*, vol. 35, no. 5, pp. 1108–1117, Oct. 1999.

[36] A. Consoli, S. Musumeci, G. Oriti, and A. Testa, "An innovative EMI reduction design technique in power converters," *IEEE Trans. Electromagn. Compat.*, vol. 38, no. 4, pp. 567–575, Nov. 1996.
[37] A. Galluzzo, M. Melito, G. Belverde, S. Musumeci, A. Raciti, and A. Testa, "Switching characteristic improvement of modern gate controlled devices," in *Proc. 5th Eur. Conf. Power Electron. Appl.*, 1993, pp. 374–379.
[38] G. Schmitt, R. Kennel, and J. Holtz, "Voltage gradient limitation of IGBTs by optimised gate-current profiles," in *Proc. 39th IEEE Power Electron. Spec. Conf.*, 2008, pp. 3592–3596.
[39] M. Rose, J. Krupar, and H. Hauswald, "Adaptive dv/dt and di/dt control for isolated gate power devices," in *Proc. 2nd IEEE Energy Convers. Congr. Expo.*, 2010, pp. 927–934.
[40] I. Baraia, J. A. Barrena, G. Abad, J. M. Canales Segade, and U. Iraola, "An experimentally verified active gate control method for the series connection of IGBT/diodes," *IEEE Trans. Power Electron.*, vol. 27, no. 2, pp. 1025–1038, Feb. 2012.
[41] B. Wittig and F. Fuchs, "Analysis and comparison of turn-off active gate control methods for low-voltage power MOSFETs with high current ratings," *IEEE Trans. Power Electron.*, vol. 27, no. 3, pp. 1632–1640, Mar. 2012.
[42] H. Kuhn, T. Koneke, and A. Mertens, "Potential of digital gate units in high power appliations," in *Proc. 13th Int. Conf. Power Electron. Motion Control*, 2008, pp. 1458–1464.
[43] M. Blank, T. Gluck, A. Kugi, and H.-P. Kreuter, "Digital slew rate and s-shape control for smart power switches to reduce EMI generation," *IEEE Trans. Power Electron.*, vol. 30, no. 9, pp. 5170–5180, Sep. 2015.
[44] L. Dang, H. Kuhn, and A. Mertens, "Digital adaptive driving strategies for high-voltage IGBTs," *IEEE Trans. Ind. Appl.*, vol. 49, no. 4, pp. 1628–1636, Jul. 2013.
[45] A. Lindberg, W. Belwon, and P. Oom, "MACS ICON - IGBT based propulsion systems," in *Proc. 1997 7th Eur. Conf. Power Electron. Appl.*, 1997, pp. 3492–3497.
[46] N. Idir, R. Bausiere, and J. J. Franchaud, "Active gate voltage control of turn-on di/dt turn-off dv/dt in insulated gate transistors," *IEEE Trans. Power Electron.*, vol. 21, no. 4, pp. 849–855, Jul. 2006.
[47] X. Yang, X. Zhang, and P. R. Palmer, "IGBT converters conducted EMI analysis by controlled multiple-slope switching waveform approximation," in *Proc. 2013 IEEE Int. Symp. Ind. Electron.*, 2013, pp. 1–6.
[48] K. Fink and S. Bernet, "Advanced gate drive unit with closed-loop dic/dt control," *IEEE Trans. Power Electron.*, vol. 28, no. 5, pp. 2587–2595, May 2013.
[49] S. Park and T. M. Jahns, "Flexible dv/dt and di/dt control method for insulated gate power switches," *IEEE Trans. Ind. Appl.*, vol. 39, no. 3, pp. 657–664, May 2003.
[50] Y. Lobsiger and J. W. Kolar, "Stability and robustness analysis of d/dt-closed-loop IGBT gate drive," in *Proc. 2013 28th Annu. IEEE Appl. Power Electron. Conf. Expo.*, 2013, pp. 2682–2689.
[51] Y. Wang, P. R. Palmer, T. C. Lim, S. J. Finney, and A. T. Bryant, "Real-time optimization of IGBT/diode cell switching under active voltage control," in *Proc. 41st IEEE Ind. Appl. Soc. Annu. Meeting*, vol. 5, 2006, pp. 2262–2268.
[52] X. Yang, Y. Yuan, Z. Long, J. Goncalves, and P. R. Palmer, "Robust stability analysis of active voltage control for high-power IGBT switching by Kharitonov's theorem," *IEEE Trans. Power Electron.*, vol. 31, no. 3, pp. 2584–2595, Mar. 2016.
[53] Y. Lobsiger and J. W. Kolar, "Closed-loop di/dt and dv/dt IGBT gate driver," *IEEE Trans. Power Electron.*, vol. 30, no. 6, pp. 3402–3417, Jun. 2015.
[54] S. Takizawa, S. Igarashi, and K. Kuroki, "A new di/dt control gate drive circuit for IGBTs to reduce EMI noise and switching losses," in *Proc. 29th Annu. IEEE Power Electron. Spec. Conf.*, vol. 2, 1998, pp. 1443–1449.
[55] J. F. Donlon, E. R. Motto, M. Honsberg, T. Radke, and T. Matsuoka, "Turn-on loss vs. free-wheel diode recovery dv/dt in IGBT modules," in *Proc. 2011 IEEE Energy Convers. Congr. Expo.*, 2011, pp. 4144–4147.
[56] W. McMurray, "Optimum snubbers for power semiconductors," *IEEE Trans. Ind. Appl.*, vol. IA-8, no. 5, pp. 593–600, Sep. 1972.
[57] W. Frank, A. Arens, and S. Hoerold, "Real-time adjustable gate current control IC solves dv/dt problems in electric drives," in *Proc. Int. Exhib. Conf. Power Electron., Intell. Motion, Renew. Energy Energy Manag.*, 2014, pp. 1–7.
[58] D. Kawase, M. Inaba, K. Horiuchi, and K. Saito, "High voltage module with low internal inductance for next chip generation-next high power density dual (nHPD2)," in *Proc. Int. Exhib. Conf. Power Electron., Intell. Motion, Renew. Energy Energy Manag.*, 2015, pp. 1–7.
[59] R. Schnell, S. Hartmann, D. Truessel, F. Fischer, A. Baschnagel, and M. Rahimo, "LinPak, a new low inductive phase-leg IGBT module with easy paralleling for high power density converter designs," in *Proc. Int. Exhib. Conf. Power Electron., Intell. Motion, Renew. Energy Energy Manag.*, 2015, pp. 1–8.
[60] E. U. Krafft, B. Laska, A. Nagel, and J. Weigel, "A new standard IGBT housing for high-power converters," in *Proc. 1997 17th Eur. Conf. Power Electron. Appl.*, 2015, pp. 1–11.
[61] P. J. Grbovic, "An IGBT gate driver for feed-forward control of turn-on losses and reverse recovery current," *IEEE Trans. Power Electron.*, vol. 23, no. 2, pp. 643–652, Mar. 2008.
[62] N. Mohan, T. M. Undeland, and W. P. Robbins, *Power Electronics: Converters, Applications, and Design*, 3rd ed. New York, NY, USA: Wiley, 2003.
[63] D.-P. Sadik *et al.*, "Short-circuit protection circuits for silicon-carbide power transistors," *IEEE Trans. Ind. Electron.*, vol. 63, no. 4, pp. 1995–2004, Apr. 2016.
[64] Y. Luo, F. Xiao, B. Wang, B. Liu, and Y. Xia, "A voltage model of PIN diodes at reverse recovery under short-time freewheeling," *IEEE Trans. Power Electron.*, vol. 32, no. 1, pp. 142–149, Jan. 2017.
[65] U.-M. Choi, F. Blaabjerg, and K.-B. Lee, "Study and handling methods of power IGBT module failures in power electronic converter systems," *IEEE Trans. Power Electron.*, vol. 30, no. 5, pp. 2517–2533, May 2015.
[66] MBM900FS17F, Datasheet from Hitachi, Spec. no. IGBT-SP-15013 R0 P1.

Erik Velander (S'14) was born in Mockfjärd, Sweden, in 1980. He received the M.Sc. degree in electrical engineering from the Chalmers University of Technology, Göteborg, Sweden, in 2006. He is currently working toward the Ph.D. degree in cooperation in the Department of Electric Power and Energy Systems, KTH Royal Institute of Technology, Stockholm, Sweden.

He has been working with high power semiconductors, gate drives, and their associated test environment for 9 years within Bombardier Transportation, Västerås, Sweden. His current research interests include gate drives for IGBTs and silicon carbide power devices aimed for traction converters.

Lennart (Zdansky) Kruse was born in Uppsala, Sweden, in 1961. He received the Master of Science degree in engineering physics from Uppsala University, Uppsala, Sweden, in 1986.

From 1986 to 1997, he was with ABB Corporate Research, Västerås, Sweden, working on MOS-controlled power semiconductors and their control. In 1997, he joined Bombardier Transportation, Västerås, Sweden, working with IGBT control, electrical insulation in converters, and type testing of converters. In 2012, he was appointed a BT Expert in power electronics.

Thomas (Lundström) Wiik was born in Södertälje, Sweden, in 1966. He received the M.Sc. degree in applied physics from the Linköping Institute of Technology, Linköping, Sweden, in 1990, and the Ph.D. degree in material science (semiconductor physics) from Linköping University, Linköping, Sweden, in 1997.

In 2009, he joined Bombardier Transportation, Västerås, Sweden, as a Component Engineer for power semiconductor devices. In 2013, he was appointed a BT expert in power electronics.

Anders Wiberg was born in Karlsborg, Sweden, in 1967. He received the B.S. degree in electrical engineering from Mälardalen University, Västerås, Sweden, in 2006.

He started with printed circuit board design at ABB. In 2008, he joined Bombardier Transportation, Västerås, Sweden, as a Traction Converter Designer, spending the recent years working mainly with traction system electrical design and associated tools.

Juan Colmenares (S'12) was born in Maracaibo, Venezuela, in 1989. He received the Diploma in electronic engineering from the Universidad Simon Bolivar, Caracas, Venezuela, in 2012, and the Ph.D. degree from the Department of Electric Power and Energy Systems, KTH Royal Institute of Technology, Stockholm, Sweden, in 2016.

His research interests include the design, manufacturing, testing, development, and reliability of power electronics systems using wide band gap (WBG) semiconductors for a wide variety of purposes. In particular, extreme implementations for WBG semiconductors, such as high efficiency converters and high temperature design using silicon carbide (SiC) power modules for automotive and aerospace applications, respectively. Additionally, new topologies as well as short-circuit protection drivers have been developed in order to fully take advantage of the SiC properties.

Hans-Peter Nee (S'91–M'96–SM'04) received the M.Sc., Licentiate, and Ph.D. degrees in electrical engineering from the KTH Royal Institute of Technology, Stockholm, Sweden, in 1987, 1992, and 1996, respectively.

In 1999, he became a Professor of power electronics in the Department of Electric Power and Energy Systems, KTH Royal Institute of Technology, Stockholm, Sweden. His research interests include power electronic converters, semiconductor components, and control aspects of utility applications, such as flexible ac transmission systems and high-voltage dc transmission, and variable-speed drives.

Dr. Nee is a member of the European Power Electronics and Drives Association, involved with the Executive Council and the International Scientific Committee. He is an Associate Editor for the IEEE TRANSACTIONS ON POWER ELECTRONICS.